Figure S1: Interphase localization of YPet-fused transcription factors and additional control immunofluorescence and SNAP-tag fusion imaging, related to Fig.1

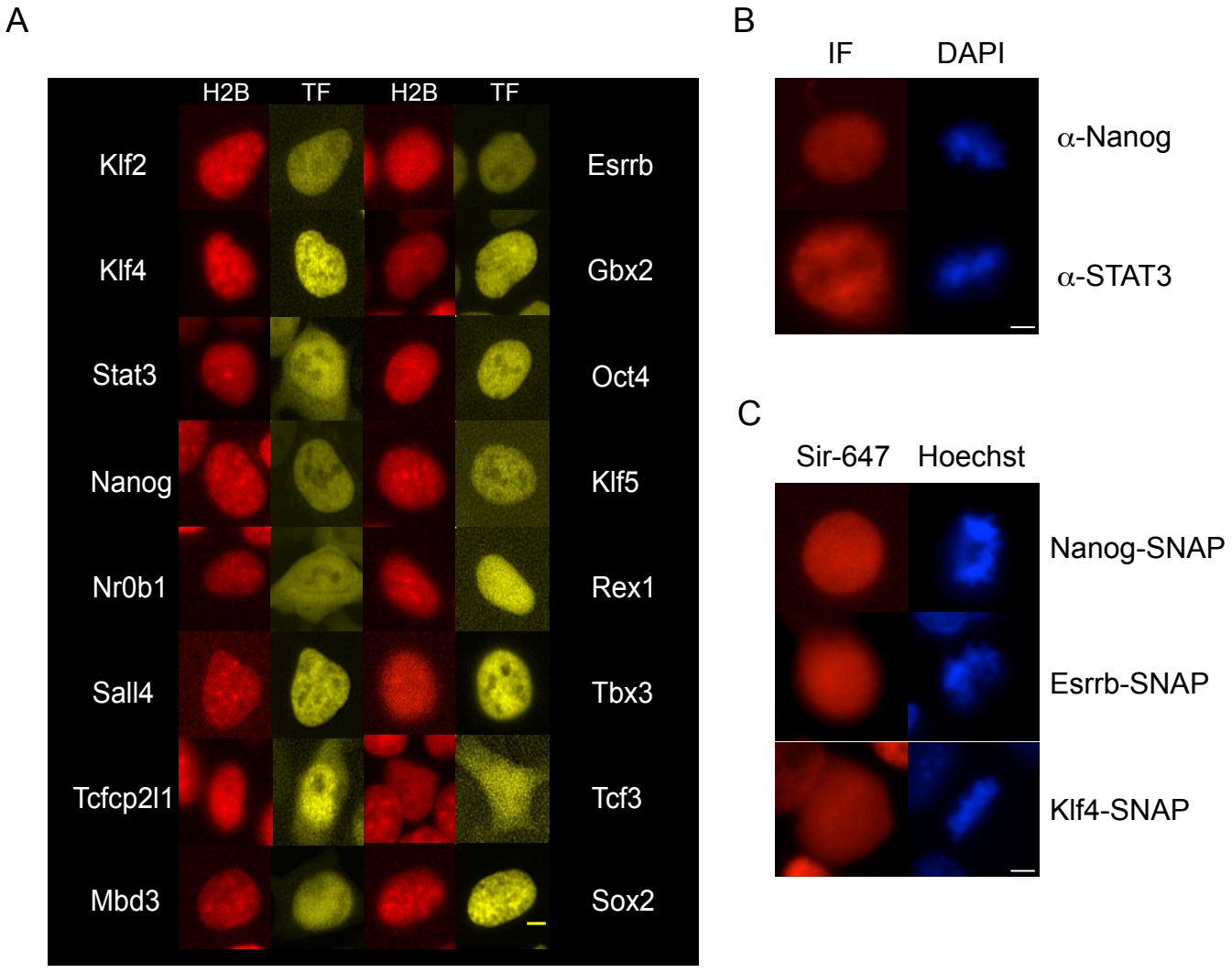

(A) Interphase localization of pluripotency transcription factors (TF) fused to Ypet. *(B)* Metaphase cells staining with a Nanog or STAT3 antibody. *(C)* Snapshots of metaphase cells of dox-inducible Esrrb-SNAP, Nanog-SNAP and Klf4-SNAP ES cell lines labeled with SNAP SiR-647 and Hoechst. Scale bars: 5μm. IF: immunofluorescence channel.

Figure S2: Confocal imaging of mitotic chromosome binding in ES cells, related to Fig.1 and 2

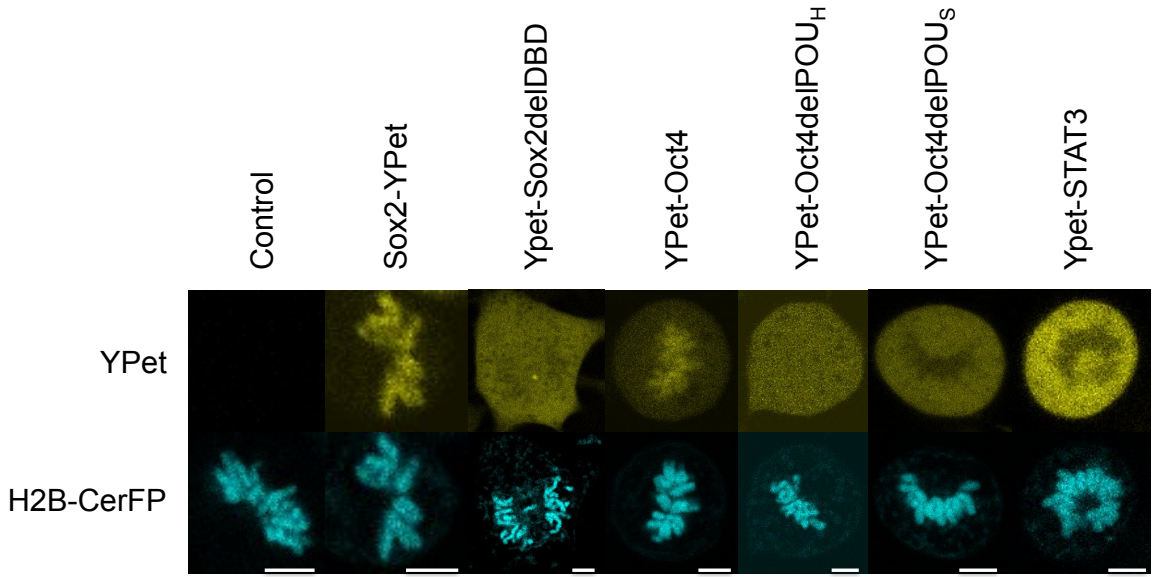

ES cell lines expressing H2BCerFP and different doxycycline-inducible YPet fusion proteins were plated on E-cadherin-coated dishes in medium containing 100ng/ml of doxycycline and imaged by confocal microscopy 24 hours later. Scale bars: 5μm.

Figure S3: Genomic analysis of Sox2-luciferase and Luciferase-Oct4 knock-in ES cells, related to Fig.1

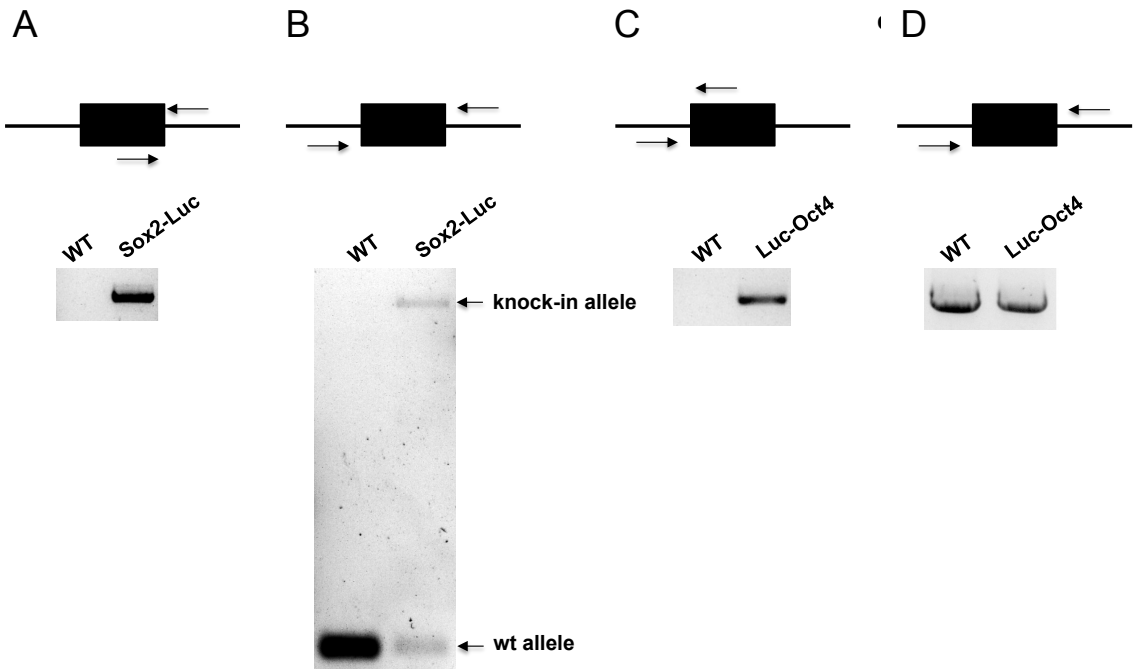

PCR analysis of the genomic insertion sites for the knock-in cassettes of Sox2-Luc *(A-B)* and Luc-Oct4 *(C-D)*. The black boxes represents the knock-in cassette with homology arms to the targeted region. The black line represents flanking genomic regions of the expected insertion sites for Sox2 and Oct4. Note that for Luc-Oct4, we were unable to amplify the whole knock-in cassette (expected product size: 5.2kb), thus only the PCR product for the wild type (wt) allele can be seen.

Figure S4: DNA residence time extraction from single molecule imaging experiments, related to Fig.4

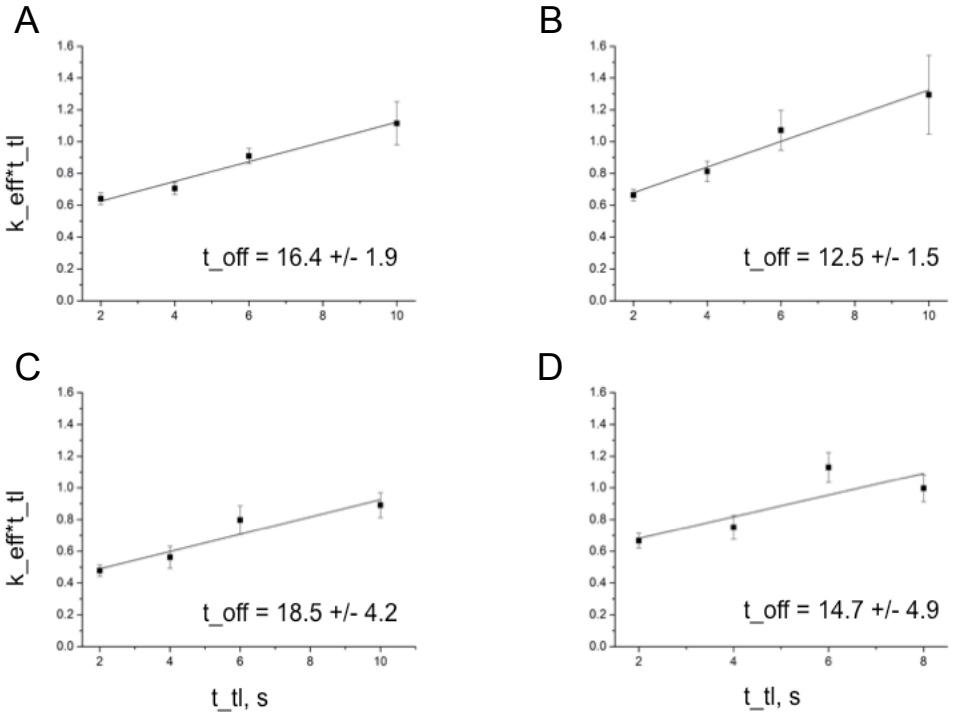

The effective residence time (t_{eff}) that we measured in single molecule tracking experiments is a function of transcription factor residence time (t_{off}) and fluorophore bleaching (t'_{bleach}):

$k_{eff} = k_{off} + k_{bleach}$;

$\frac{1}{t_{eff}} = \frac{1}{t_{off}} + \frac{1}{t'_{bleach}}$;

As we vary the dark time, or gaps between images (t_{gap}), fluorophore bleaching (t'_{bleach}) and the effective residence time (t_{eff}) vary with a rate that depends on the time-lapse parameters (t_{int} - image acquisition time):

$t_{tl} = t_{int} + t_{gap}$, $t_{int} = 2\ s\ (const)$;

$t'_{bleach} = \frac{t_{tl}}{t_{int}} t_{bleach}$, $t_{bleach} = (const)$;

$\frac{1}{t_{eff}} = \frac{1}{t_{off}} + \frac{t_{int}}{t_{tl}} \frac{1}{t_{bleach}}$;

Measuring the effective binding time for different gap conditions thus allows us to extract the true binding time t_{off} as a linear regression coefficient according to the equation below.

$k_{eff} t_{tl} = \frac{1}{t_{off}} t_{tl} + \frac{1}{t_{bleach}} t_{int}$;

as shown here for *(A)* Sox2 in interphase; *(B)* Sox2 in M-phase; *(C)* Oct4 in interphase; *(D)* Oct4 in M-phase. N≥3 for each t_tl condition condition.

Figure S5: Quality control of mitotic cell sorting and chromatin fragmentation, related to Fig.5

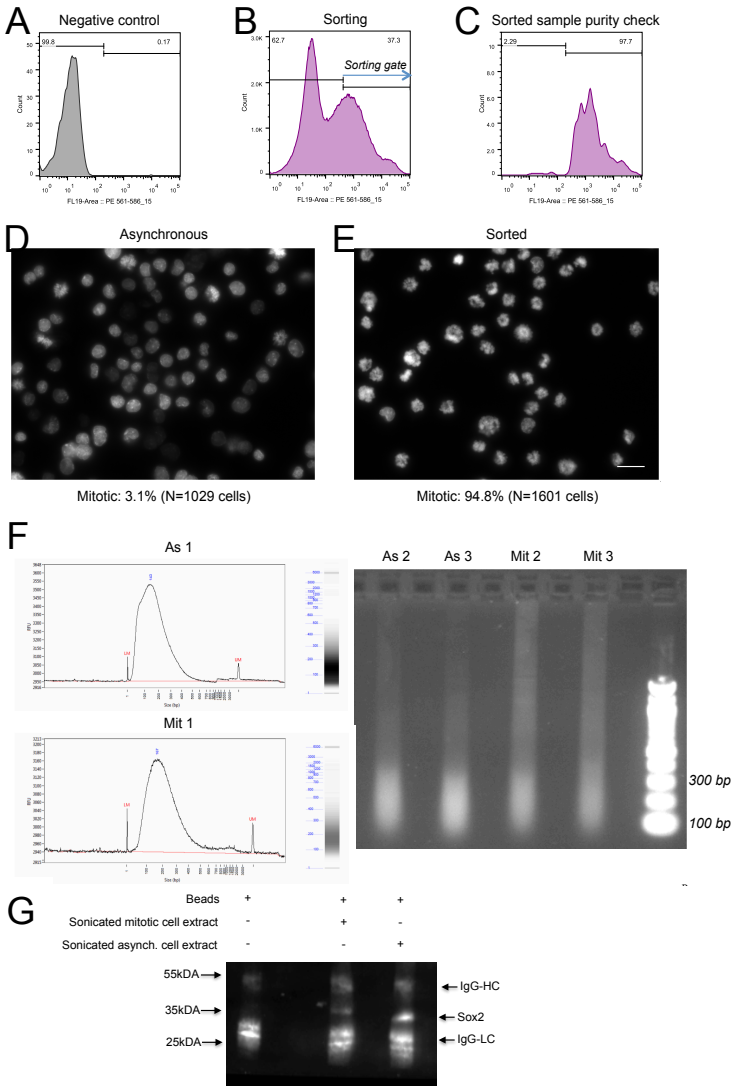

(A) Negative control cells stained with secondary antibody alone. *(B)* Sorting window for H3S10^{P}-positive cells after nocodazole synchronization. *(C)* Reanalysis of sorted sample to determine the purity of H3S10^{P}-positive cells (97.7%). *(D-E)* DAPI staining of asynchronous *(D)* and H3S10^{P}-sorted cells *(E)* to quantify the fraction of mitotic cells with condensed chromatin. Scale bar: 20 µm. *(F)* Sonication profiles of fragmented chromatin from asynchronous (As) and sorted mitotic (Mit) cells used for downstream ChIP-seq experiments. The first replicate for each condition was analyzed on a Fragment Analyzer and the two remaining replicates on a 1% agarose gel. *(G)* Western blotting against Sox2 after boiling antibody-bound beads incubated with sonicated extracts from mitotic or asynchronous cells. Antibody-bound beads were used as negative control. LC: light chains; HC: heavy chains.

Figure S6: Peak calling and selection, related to Fig.5

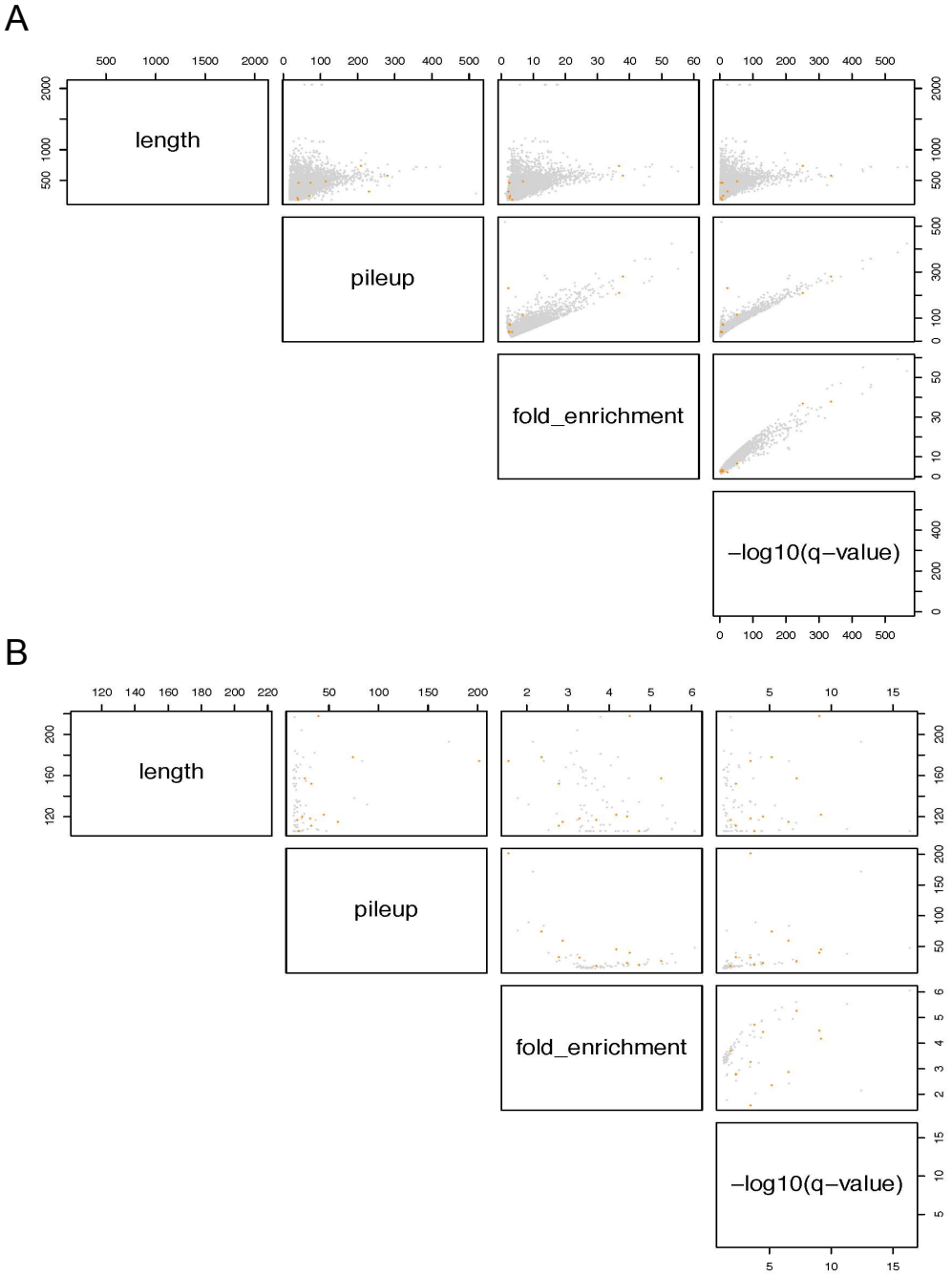

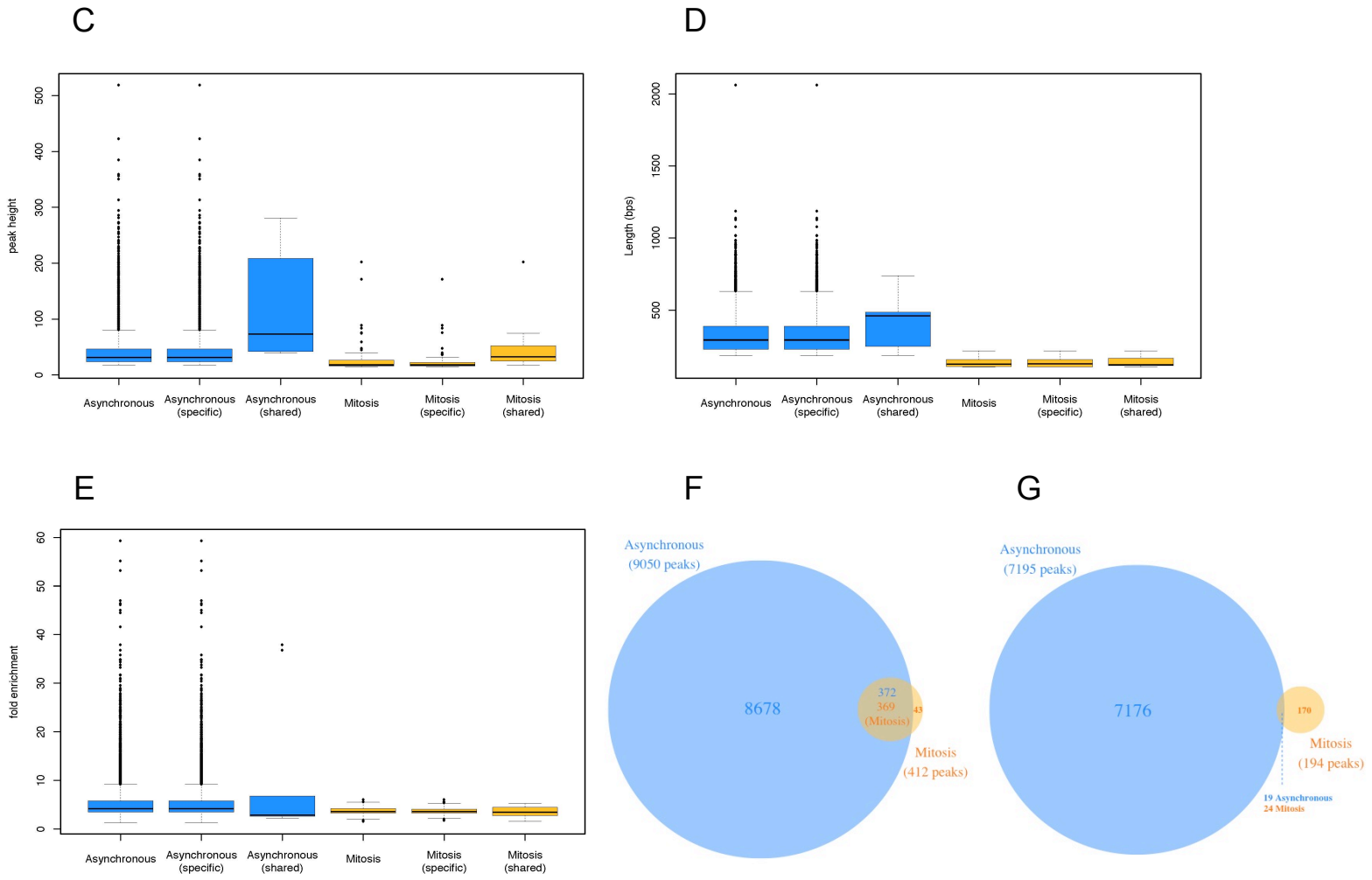

(A-B) Peak characteristics of asynchronous *(A)* and mitotic *(B)* ChIP-seq samples. Gray: selected peaks; Red: blacklisted peaks. *(C-E)* 25th-75th percentile box-plots of peak height *(C)*, peak lengths *(D)*, and peak fold-enrichment *(E)* of different classes of peaks as indicated on the x-axis. Whiskers: 1/-1.5 IQR; black line: median. *(F-G)* Number of asynchronous and mitotic peaks detected for FoxA1 (Caravaca et al. 2013) *(F)* and GATA1 (Kadauke et al.) *(G)* using our analytical pipeline.

Figure S7: Relative enrichment of called peaks, related to Fig.5

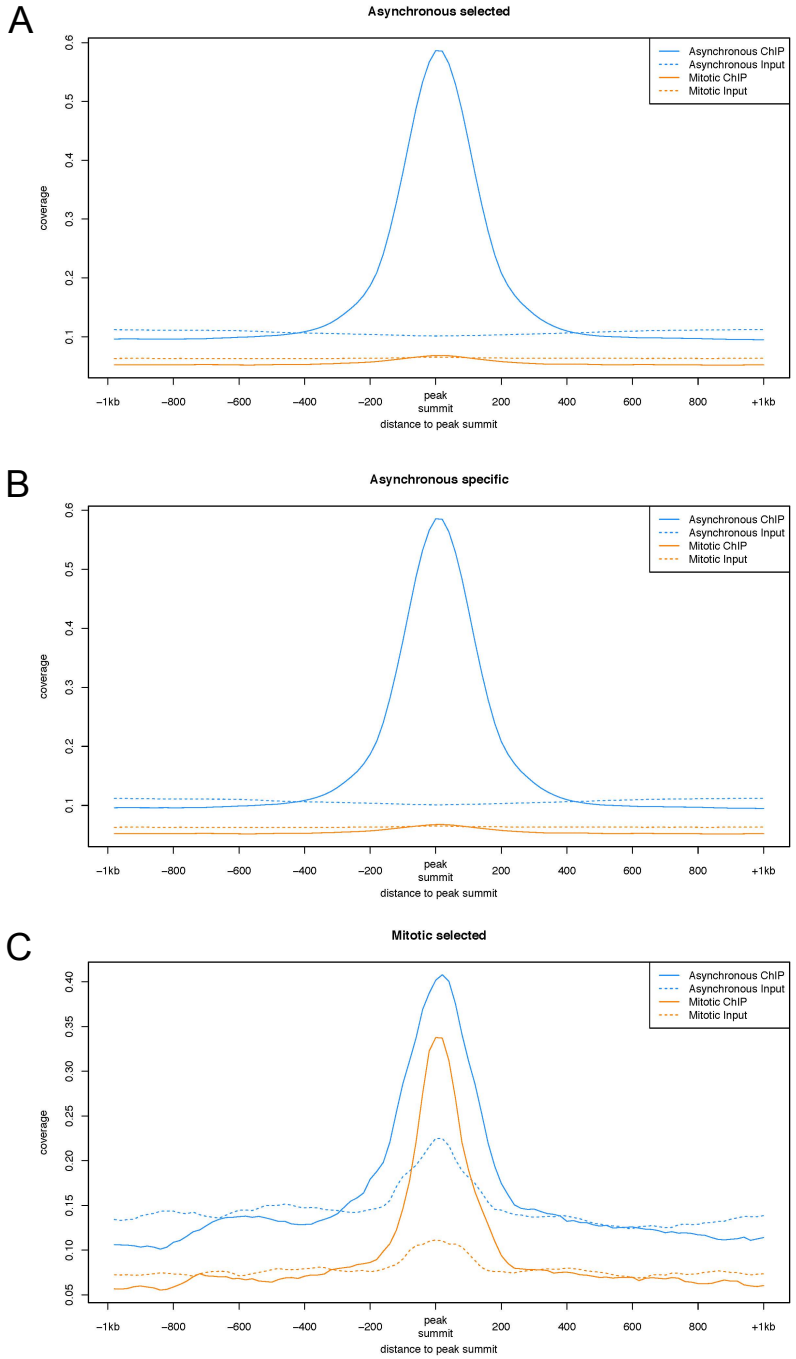

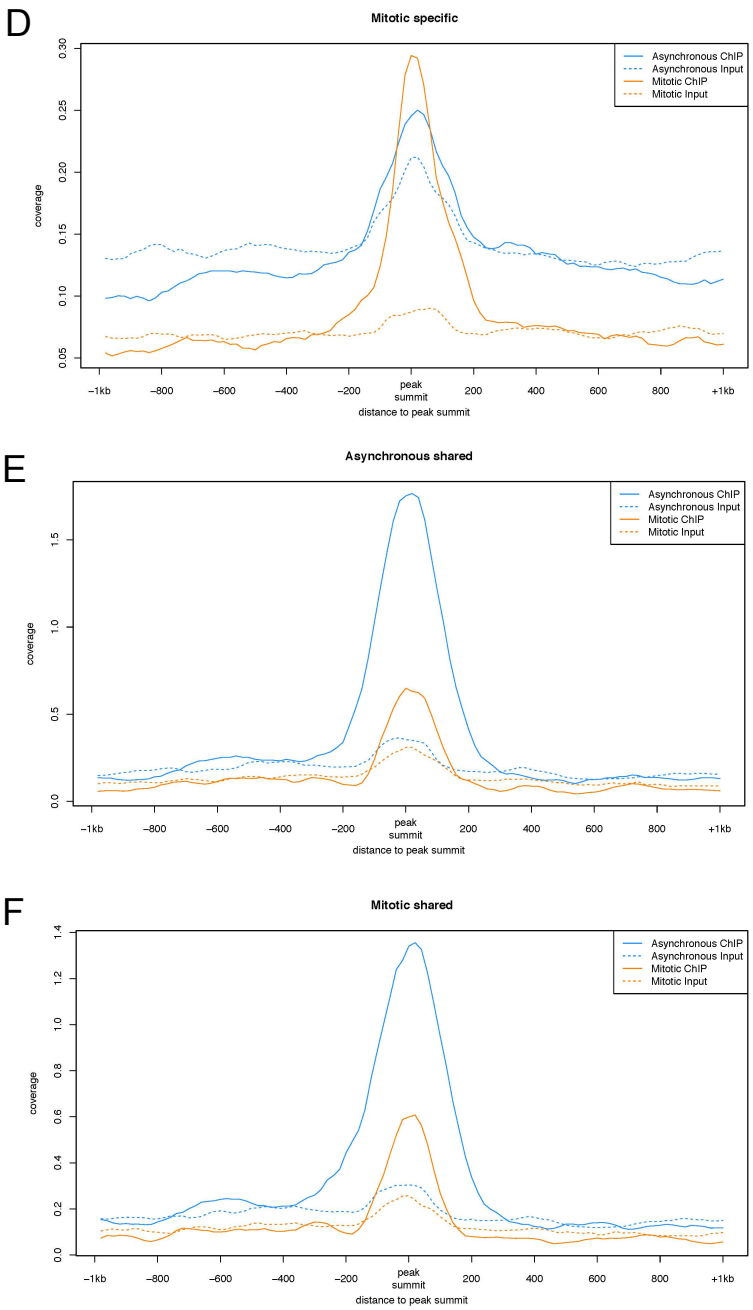

(A-B) Peak characteristics of asynchronous *(A)* and mitotic *(B)* ChiP-seq samples. Gray: selected peaks; Red: blacklisted peaks. *(C-E)* 25th-75th percentile box-plots of peak height *(C)*, peak lengths *(D)*, and peak fold-enrichment *(E)* of different classes of peaks as indicated on the x-axis. Whiskers: +/-1.5 IQR; black line: median.

Figure S8: ChIP-QPCR on selected peaks and negative control regions, related to Fig.5

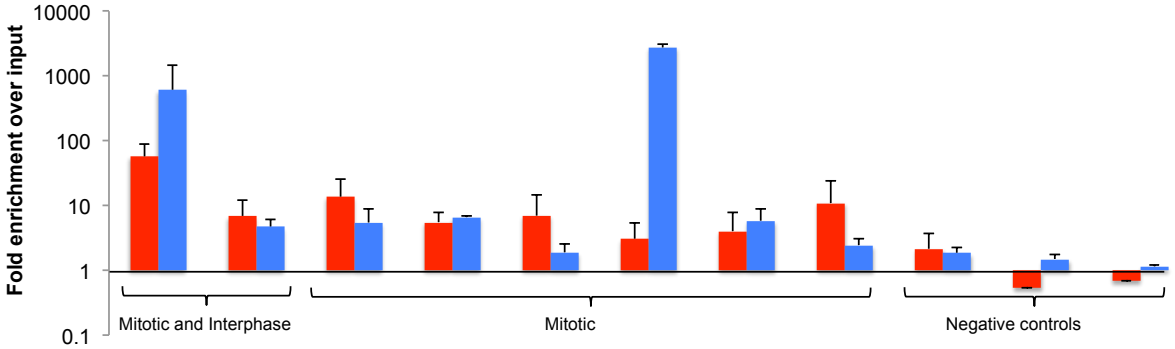

QPCR primers were designed around the center of peaks called by MACS2, for 2 peaks common to mitotic and asynchronous samples, 6 peaks called only in mitosis, and 3 regions were no peaks were called. Red: Asynchronous ChIP, N=2. Blue: Mitotic ChIP, N=2. Error bars: SE. The primer pairs used for amplification are listed in Table S3.

Figure S9: Genome-wide distribution of ChIP-seq peaks, related to Fig.5

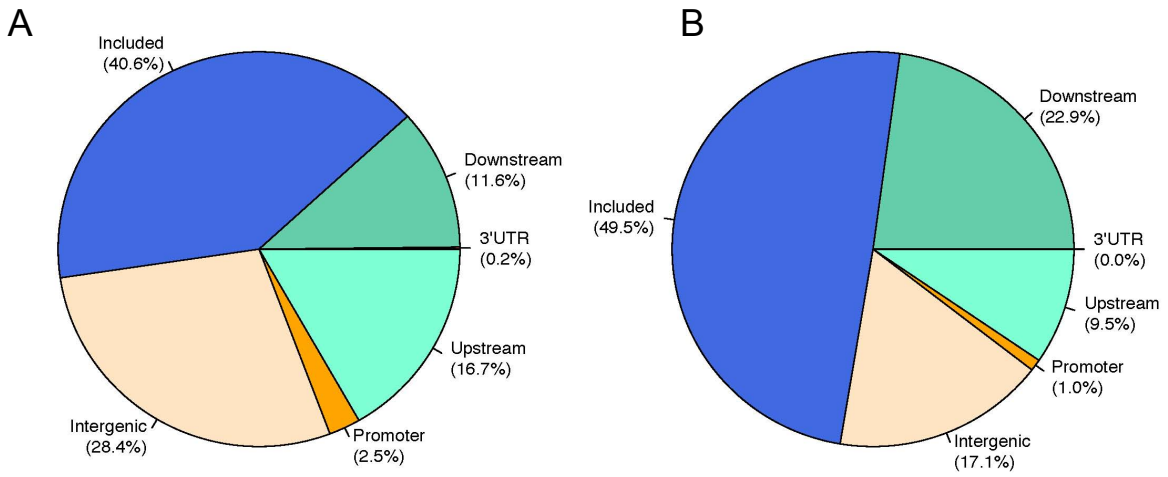

(A) Asynchronous samples. *(B)* Mitotic samples. Intergenic: regions without genes within a distance of 20kb; Promoter regions: upstream and within 2kb of the gene start; Upstream: between 2kb and 20kb upstream of transcription start sites; Included: within genes; 3'UTR: downstream and within 10% of the distance to the next downstream gene; Downstream: downstream of 3'UTR but at a distance of < 20kb to the closest downstream gene.

Figure S10: De novo motif identification with MEME in the asynchronous sample, related to Fig.5

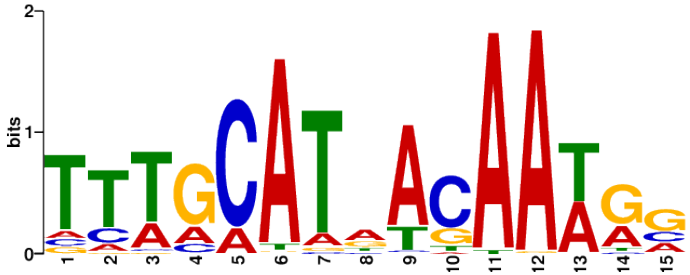

Top-scoring motif in the asynchronous samples, centered on peaks, matching the known Oct4::Sox2 composite binding motif (e-value = $4.1*10^{-343}$).

Figure S11: Sorting strategies for the Sox2 overexpressing cell lines, related to Fig.6 and Fig.7

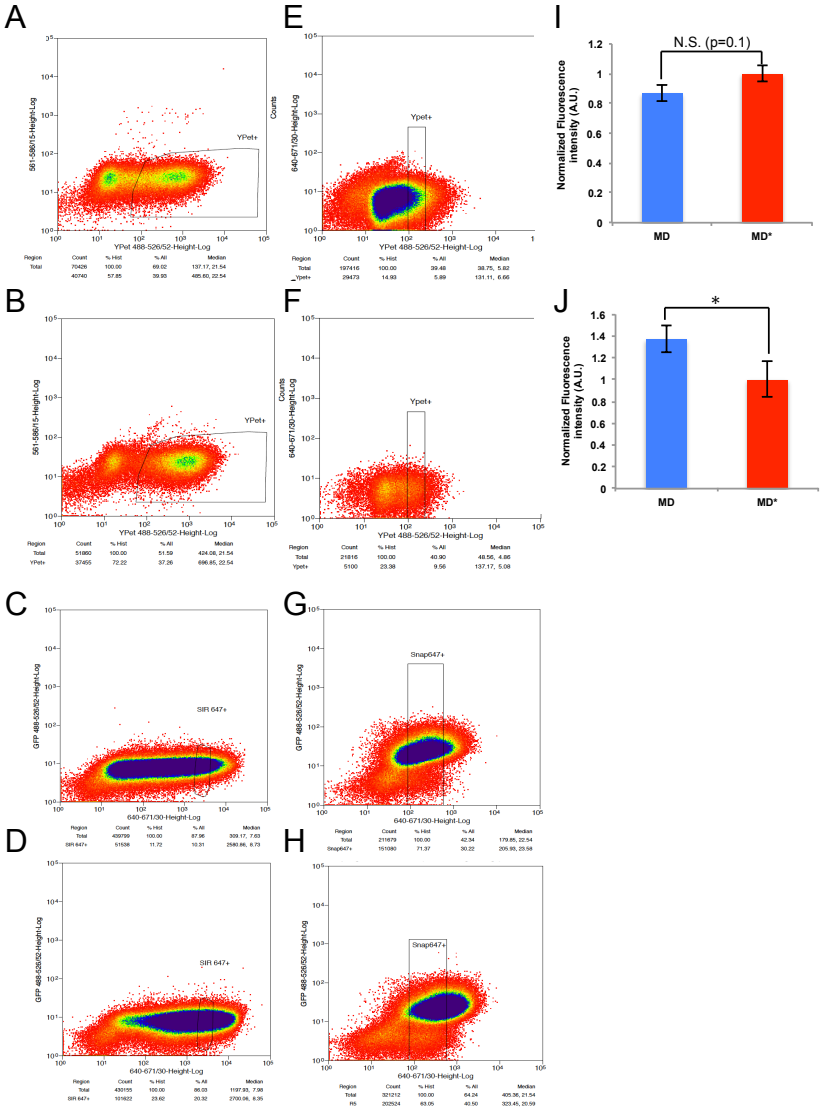

(A-H) Sorting windows of the different cell lines by FACS. *(A)* TRE3G-Sox2-YPet-MD *(B)* TRE3G-Sox2-YPet-MD*. *(C)* TRE3G-SNAP-MD-Sox2. *(D)* TRE3G-SNAP-MD*-Sox2. *(E)* PGK-Sox2-YPet-MD. *(F)* PGK-Sox2-YPet-MD*. *(G)* PGK-SNAP-MD-Sox2. *(H)* PGK-SNAP-MD*-Sox2. *(I-J)*: Integrated fluorescence intensity of cells was measured from time-lapse experiments, 5 frames =25 minutes before the condensation of chromosomes became visible, using cells that were FACS-sorted using the fluorescence windows shown in *(A)*, *(B)*, *(C)* and *(D)*. Intensities were normalized on the MD* data. Statistical analysis was performed using student's two-tailed t-test with unequal variance. *(I)* TRE3G-Sox2-YPet-MD (MD; N= 105) and TRE3G-Sox2-YPet-MD* (MD*; N=109). *(J)* TRE3G-SNAP-MD-Sox2 (MD; N=100) and TRE3G-SNAP-MD*-Sox2 (MD*; N=102). *:$p<0.05$

Figure S12: Genomic analysis of Sox1-P2A-eGFP / Brachyury-P2A-mCherry knock-in ES cells, related to Fig.7

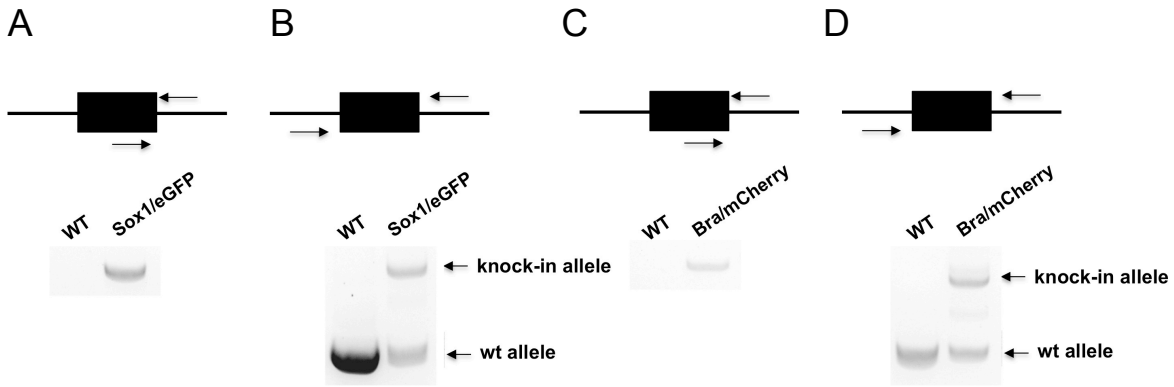

PCR analysis of the genomic insertion sites for the knock-in cassettes of Sox1-P2A-eGFP (Sox1/eGFP) *(A-B)* and Brachyury-P2A-mCherry (Bra/mCherry) *(C-D)* in the SBR cell line. The black boxes represent the knock-in cassette with homology arms to the targeted region. The black line represents flanking genomic regions of the expected insertion sites for Sox1 and Bra.